Variable-Temperature Emission Studies of Solvation Dynamics: Evidence for Coupling of Solvation to Chromophore Structural Dynamics in the Evolution of Charge-Transfer Excited States

Niels H. Damrauer and James K. McCusker*

Department of Chemistry, University of California at Berkeley, Berkeley, California 94720-1460

Received June 15, 1999

Variable-temperature emission data over the range 90−298 K have been collected for a series of bipyridyl complexes of Ru^{II}. Spectra obtained for $[Ru(dmb)_3]^{2+}$ (dmb = 4,4′-dimethyl-2,2′-bipyridine), $[Ru(dpb)_3]^{2+}$ (dpb = 4,4′-diphenyl-2,2′-bipyridine), $[Ru(dotb)_3]^{2+}$ (dotb = 4,4′-di-*o*-tolyl-2,2′-bipyridine), and $[Ru(dmesb)_3]^{2+}$ (dmesb = 4,4′-dimesityl-2,2′-bipyridine) in 4:1 EtOH/MeOH show similar trends in terms of both the red shift of the emission spectrum and the thermal breadth of the solvent response as the temperature is increased through the glass-to-fluid transition. In contrast, data collected in 2-MeTHF show a strong dependence on the identity of the chromophore, the details of the spectral evolution qualitatively correlating with changes in the steric demands of the system. The most dramatic effect is observed for $[Ru(dmesb)_3]^{2+}$, in which there is an apparent change in the nature of the emitting species with increasing temperature. These observations suggest a strong coupling of solvation dynamics and solute structure in the low-temperature regime as well as at intermediate temperatures where the structure of the chromophore is evolving in the course of excited-state relaxation. The results underscore the potential importance of specific solvent−solute interactions in the dynamics of solvation for cases in which large-amplitude molecular motion of the chromophore accompanies thermalization of the excited state.

Introduction

The study of chemical dynamics in the condensed phase has spawned tremendous interest in the role of the surrounding medium in processes ranging from small-molecule fluorescence to electron transfer in proteins.[1−3] In addition, the outer-sphere contributions to reorganization energy can be of overriding importance in governing the rate of intermolecular electron-transfer processes.[4−7] The experimental method of choice for studying solvation dynamics is usually ultrafast emission spectroscopy: the idea behind this technique is represented in Scheme 1. A chromophore dissolved in the solvent of interest is perturbed with a δ-function excitation (e.g., an ultrashort laser pulse) instantaneously altering the charge distribution within the molecule.[8] On the basis of the Franck−Condon principle, the positions of the nuclei remain unchanged during this transition. The solvation shell, still in the equilibrium configuration appropriate for the solute's ground-state charge distribution, will then begin to evolve toward a configuration that stabilizes the excited-state charge distribution. The experimental observable for these solvent dynamics is the evolution of the emission spectrum of the fluorophore itself, specifically in the energy of the fluorescence transition.

The vast majority of studies published to date have employed organic fluorophores (e.g., Coumarin 102) that have a large dipole moment change upon photoexcitation but do not undergo significant excited-state geometric distortion. The dynamics that are probed are therefore primarily due to processes associated with solvent relaxation. However, recent efforts have begun to focus on the nature of specific solute−solvent interactions, addressing such questions as how solvent responds to more complex charge distributions within a solute molecule[9] as well as how solvent molecules exert specific frictional forces on rotational motion of solute molecules.[10,11] An interesting question, therefore, is how specific solute−solvent interactions may manifest themselves in terms of coupling solvation dynamics with intramolecular excited-state dynamics such as excited-state nuclear motion. It is in this context that we have investigated certain transition metal charge-transfer chromophores. Conceptually, these types of metal complexes offer similarities to organic fluorophores used in traditional studies of solvent dynamics; i.e., absorption of light results in a large dipole moment change within the molecule around which the solvent must relax. The advantage of using transition metal complexes lies in the synthetic flexibility for tuning molecular properties that may influence the processes of solvation.[12−14] In certain circumstances such as those discussed within this paper, this motion may couple to solvation, resulting in drastic changes to the excited-state emissive properties of the chromophore itself.

(1) Maroncelli, M. *J. Mol. Liq.* **1993**, *57*, 1.
(2) Stratt, R. M.; Maroncelli, M. *J. Phys. Chem.* **1996**, *100*, 12981.
(3) Horng, M. L.; Gardecki, J. A.; Papazyan, A.; Maroncelli, M. *J. Phys. Chem.* **1995**, *99*, 17311.
(4) Chen, P. Y.; Meyer, T. J. *Chem. Rev.* **1998**, *98*, 1439.
(5) Barbara, P. F.; Walker, G. C.; Smith, T. P. *Science* **1992**, *256*, 975.
(6) Heitele, H. *Angew. Chem., Int. Ed. Engl.* **1993**, *32*, 359.
(7) Weaver, M. J.; McManis, G. E. *Acc. Chem. Res.* **1990**, *23*, 294.
(8) The ability to study dynamical processes is dependent on the time resolution of the laser pulses being used (e.g., 20 ps in TCSPC versus 20 fs in fluorescence up-conversion).
(9) Ladanyi, B. M.; Maroncelli, M. *J. Chem. Phys.* **1998**, *109*, 3204.
(10) Elich, K.; Kitazawa, M.; Okada, T.; Wortmann, R. *J. Phys. Chem. A* **1997**, *101*, 2010.
(11) Kurnikova, M. G.; Balabai, N.; Waldeck, D. H.; Coalson, R. D. *J. Am. Chem. Soc.* **1998**, *120*, 6121.

10.1021/ic990703l CCC: $18.00
Published on Web 08/28/1999

Scheme 1

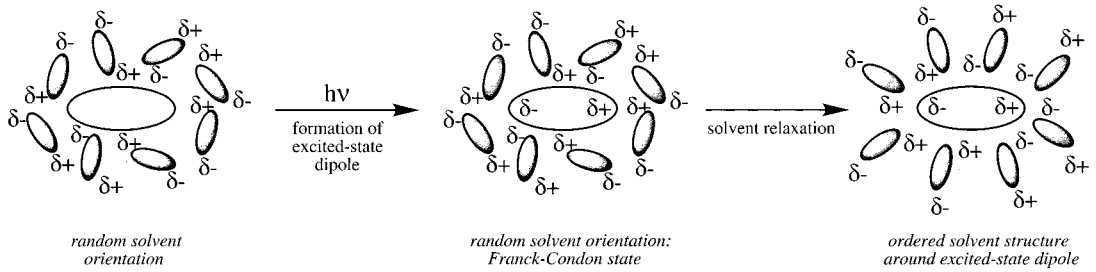

Unfortunately, although work by Barbara[15,16] and Woodruff,[17,18] as well as our own work on $[Ru(bpy)_3]^{2+}$ [19] and $[Ru(dpb)_3]^{2+}$,[20,21] points to the importance of solvation dynamics in coupling to ultrafast internal conversion and/or intersystem crossing in metal-based chromophores, the study of ultrafast solvation dynamics involving transition metal complexes is limited in certain fundamental ways. The most detrimental concerns the radiative decay rate (k_r) for emission. To capture the inertial component of the solvent response (or any process influencing emission on a time scale of <20 ps), the technique of fluorescence up-conversion is typically used. Whereas the emissive photon flux from organic dyes is often sufficient to achieve this up-conversion, the k_r values for most transition metal luminophores in fluid solution are a factor of 10^3-10^5 smaller than those for their organic counterparts. A second problem is a general inability to directly excite into the emissive state of the metal chromophore. Unlike fluorescence from organic dyes, emission from transition metal chromophores is almost invariably phosphorescent. Excitation, therefore, usually occurs into a state other than the emissive one, implying that some unknown fraction of the solvation process will go unobserved as the system evolves from the Franck−Condon state to the emissive state.

Although the traditional techniques for studying solvation dynamics do not appear to be readily applicable to transition metal complexes, information about solvation dynamics occurring in these systems can be gleaned from variable-temperature static emission spectroscopy. Here, we take advantage of the conceptual correlation one can draw between time and temperature with respect to molecular motion. This is most easily visualized using the potential energy diagram shown in Figure 1. The *x* axis in this figure is the solvent coordinate and corresponds to the collective motion of the solvation shell of the chromophore. At low temperatures, in which the solvent has either frozen or formed an optical glass, excitation onto and subsequent relaxation from the excited-state surface occur with no motion along the solvent coordinate: both excitation and emission therefore occur vertically on this diagram. This can be likened to an extremely short time scale measurement in which no large-amplitude motion of the solvent has occurred and relaxation from the excited state takes place from the equilibrium solvent configuration of the ground state. As the temperature is increased (e.g., through the glass-to-fluid transition, T_g) the solvent molecules will begin to move, just as increasing the time delay from $t = 0$ to $t > 0$ in a time-resolved experiment allows one to begin probing molecular motion of the solvent. In this intermediate-temperature regime, relaxation from the excited-state surface occurs on approximately the same time scale as motion along the solvent coordinate. The experimental manifestation of this evolution for the time-integrated variable-temperature spectra is a red shift, analogous to that seen in the time-resolved experiment. Finally, at sufficiently high temperatures (sufficiently long time delay), the kinetics of solvation are rapid compared to the kinetics of ground-state recovery. This corresponds to the steady-state condition. Thus, at least in a qualitative sense, the entire path along the solvent coordinate potential surface is sampled in both experiments, given a sufficiently wide thermal or temporal range.

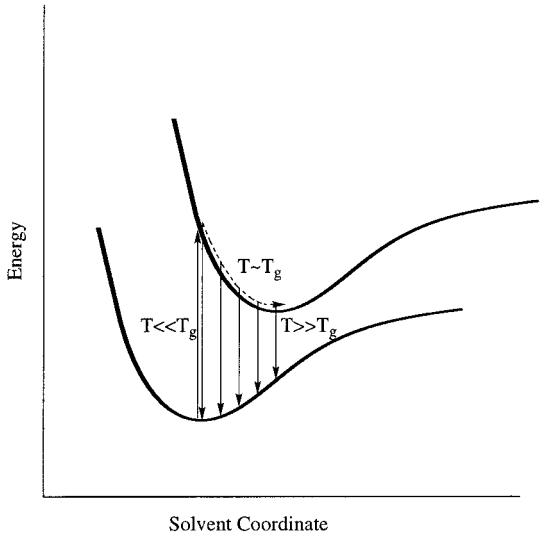

Figure 1. Potential energy surface diagram for energy versus solvent coordinate showing various emissive transitions for a rigid glass ($T < T_g$) versus fluid solution ($T > T_g$).

We previously reported[14,22] the molecular dynamics associated with excited-state evolution in a series of aryl-substituted

(12) It is possible to manipulate the energetics of absorption, to influence the size of the excited-state dipole that is formed upon excitation, and/or to introduce ligands that undergo photoinduced excited-state nuclear motion via synthetic modifications to the system. (cf. refs 13 and 14)
(13) Juris, A.; Balzani, V.; Barigelletti, F.; Campagna, S.; Belser, P.; Von Zelewsky, A. *Coord. Chem. Rev.* **1988**, *84*, 85.
(14) Damrauer, N. H.; Boussie, T. R.; Devenney, M.; McCusker, J. K. *J. Am. Chem. Soc.* **1997**, *119*, 8253.
(15) Reid, P. J.; Silva, C.; Barbara, P. F.; Karki, L.; Hupp, J. T. *J. Phys. Chem.* **1995**, *99*, 2609.
(16) Olson, E. J. C.; Hu, D.; Hormann, A.; Jonkman, A. M.; Arkin, M. R.; Stemp, E. D. A.; Barton, J. K.; Barbara, P. F. *J. Am. Chem. Soc.* **1997**, *119*, 11458.
(17) Doorn, S. K.; Stoutland, P. O.; Dyer, R. B.; Woodruff, W. H. *J. Am. Chem. Soc.* **1992**, *114*, 3133.
(18) Doorn, S. K.; Dyer, R. B.; Stoutland, P. O.; Woodruff, W. H. *J. Am. Chem. Soc.* **1993**, *115*, 6398.
(19) Damrauer, N. H.; Cerullo, G.; Yeh, A.; Boussie, T. R.; Shank, C. V.; McCusker, J. K. *Science* **1997**, *275*, 54.
(20) Damrauer, N. H.; McCusker, J. K. *J. Phys. Chem. A*, in press.
(21) Damrauer, N. H.; Curtright, A. E.; McCusker, J. K. Manuscript in preparation.
(22) Damrauer, N. H.; Weldon, B. T.; McCusker, J. K. *J. Phys. Chem. A* **1998**, *102*, 3382.

bipyridyl complexes of the general form $[Ru(L)_3]^{2+}$(the dpb series), where L is 4,4′-diphenyl-2,2′-bipyridine (dpb), 4,4′-di-*o*-tolyl-2,2′-bipyridine (dotb), or 4,4-dimesityl-2,2′-bipyridine (dmesb). A combination of static and nanosecond time-resolved

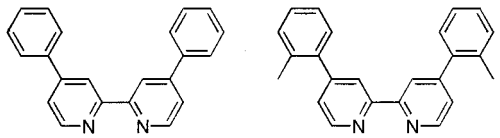

dpb *dotb*

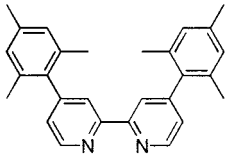

dmesb

absorption, emission, and resonance Raman spectroscopies helped to establish a simple model in which rotation of the aryl substituent was proposed to be strongly coupled to thermalization of the emissive ^{3}MLCT excited state(s) of these compounds,[14] e.g., for $[Ru(dpb)_3]^{2+}$

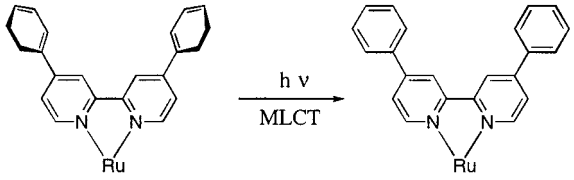

canted *planar*

These experimental studies were supported by computational efforts[22] that further elucidated the nature of both the thermalized ^{3}MLCT excited state and the Franck−Condon state as a prelude to ultrafast studies of electron delocalization.[20,21] Given the large-amplitude motion involved in the thermalization of these complexes, it occurred to us that the solvent might play an important role in the excited-state dynamics. Herein, we report results from a variable-temperature static emission study designed to probe the interplay between solvation and molecular dynamics in $[Ru(dpb)_3]^{2+}$, $[Ru(dotb)_3]^{2+}$, and $[Ru(dmesb)_3]^{2+}$, using 4:1 EtOH/MeOH and 2-MeTHF as comparative solvents.

Experimental Section

General Materials and Procedures. All reagents and materials from commercial sources were used as received unless otherwise noted. Solvents were purchased from either Aldrich Chemical Co. or Fisher. The ligands 4,4′-dimethyl-2,2′-bipyridine (dmb) and 4,4′-diphenyl-2,2′-bipyridine (dpb) were purchased from Aldrich Chemical Co. The ligands 4,4′-di-*o*-tolyl-2,2′-bipyridine (dotb) and 4,4′-dimesityl-2,2′-bipyridine (dmesb) and the metal complexes $[Ru(dmb)_3](PF_6)_2$, $[Ru(dpb)_3](PF_6)_2$, $[Ru(dotb)_3](PF_6)_2$, and $[Ru(dmesb)_3](PF_6)_2$ were prepared according to previously published procedures.[14] $[Ru(dmb)_3]Cl_2$ was prepared via standard methods. The tetrakis(fluoroaryl)borate (BArF) counterion was generously donated by Dr. Thomas Boussie of Symyx Technologies as the sodium salt, NaB(3,5-bis(trifluoromethyl)phenyl)$_4$. No further purification was necessary.

Metathesis of $[Ru(dmb)_3]Cl_2$ to $[Ru(dmb)_3](BArF)_2$. $[Ru(dmb)_3]Cl_2$ (164 mg, 0.227 mmol) was dissolved in water and a minimal amount of EtOH. To this was added a 1:1 water/methanol solution of NaBArF (402 mg, 0.454 mmol), resulting in the formation of an insoluble orange solid, which was filtered off, washed with water, and collected to yield the BArF salt as an orange powder. This compound was then recrystallized twice by diffusion of hexanes into ethanol. Anal. Calcd for $C_{100}H_{60}B_2F_{48}N_6Ru$: C, 50.46; H, 2.54; N, 3.53. Found: C, 50.85; H, 2.76; N, 3.82. MS (ES): *m*/*z* 1517 ($[M - BArF]^+$, 50%), 327 ($[M - 2BArF]^{2+}$, 100%).

Physical Measurements. Variable-Temperature Emission Spectra. Emission spectra were collected using an Instruments SA/Jobin Yvon-Spex Fluoromax photon-counting fluorimeter. The equipment and general methodology for collecting and correcting data were previously described.[14]

Samples were prepared in an Ar atmosphere drybox. Two solvent systems were used for measurements: 2-methyltetrahydrofuran (2-MeTHF) and 4:1 ethanol/methanol (4:1 EtOH/MeOH). Solvents brought into the box were thoroughly deoxygenated with four freeze−pump−thaw cycles. 2-MeTHF was freshly distilled from CaH_2 prior to each use due to the formation of an emissive decomposition impurity upon sitting in the drybox for multiple days. Ethanol and methanol were distilled from $MgSO_4$, deoxygenated, and brought into the drybox separately. There, they were combined in the 4:1 EtOH/MeOH proportion used for variable-temperature measurements.

Each sample was prepared optically thin (o.d. $\sim$ 0.1) in a 1 cm wide glass test tube (Fisher Scientific). A rubber septum was placed over the tube before removing the sample from the drybox. Outside the drybox, the sample was immediately frozen with liquid nitrogen and the test tube was then flame-sealed. The sample was warmed to room temperature and fit in a home-built holder attached to the sample positioner assembly of a Janis model SVT Research Cryostat outfitted with optical windows. Emission measurements were taken with this optical dewar mounted within the sample chamber of the fluorimeter. Emission was collected at 90° from the single-wavelength 450 nm excitation beam. The dewar is designed to allow for sample temperature control from 1.5 to 300 K; however, using liquid nitrogen in both the inner and outer chambers of the dewar allowed for sample temperature control from 90 K to room temperature. In this configuration, flowing gaseous nitrogen from a liquid nitrogen reservoir is passed over the sample. The temperature of the sample was manipulated by controlling the temperature of this gas with two Lake Shore model 321-01 temperature controllers, two silicon diode temperature sensors, and two 25 Ω wound resistive heaters. One of the two silicon diodes and one of the two resistive heaters are permanent fixtures within the dewar and sit approximately 1 in. from the bottom of the sample. The second diode and resistive heater sit approximately 2 in. above the sample on the sample positioner assembly. With simultaneous feedback control of the two resistive heaters surrounding the sample, temperature control was obtained with a precision of better than ±0.1 K.

Variable-temperature measurements were made as follows: Each sample was cooled to 90 K and allowed to stabilize such that each of the two temperature controllers reading the silicon diode temperature sensors agreed to within ±0.1 K with little fluctuation. A fluorescence spectrum was then collected, and the temperature of the sample was increased. Typically, this was done in a 10 K increment with the exception of certain regions for the $[Ru(dmesb)_3]^{2+}$ sample for which $\Delta T = 5$ K. The sample was allowed to stabilize at the new temperature to within ±0.1 K (typically requiring approximately 20 min), and a new fluorescence spectrum was taken. This process was repeated until the highest temperature spectrum had been taken. Care was taken to avoid moving the optical dewar within a full variable-temperature run to ensure that small alignment changes, which might cause variations in spectral intensity, did not occur.

Results and Discussion

I. Variable-Temperature Studies in 4:1 EtOH/MeOH. Spectral Changes for $[Ru(dmb)_3]^{2+}$. Emission spectra collected for $[Ru(dmb)_3]^{2+}$ in 4:1 EtOH/MeOH in the range from 90 to 298 K are essentially identical in profile to those reported in the literature for $[Ru(bpy)_3]^{2+}$ and similar members of this class of molecules[23−26] and can be found in the Supporting Information. As the temperature is lowered from room temper-

(23) Hager, G. D.; Crosby, G. A. *J. Am. Chem. Soc.* **1975**, *97*, 7031.

ature to 90 K, we observe a marked increase in intensity,[27,28] the introduction of fine structure,[29] and a significant blue shift of the spectrum. For our purposes, the most important characteristic of the variable-temperature spectra is the substantial blue shift one observes upon formation of the optical glass. In the case of $[Ru(dmb)_3]^{2+}$, the emission maximum shifts by 1000 cm^{-1} from 15 900 cm^{-1} at 298 K to 16 900 cm^{-1} at 100 K; below this temperature, we see no further change in the position of the spectrum. The spectra undergo most of the shift over a relatively narrow temperature range (ca. 100−130 K) such that the changes appear to track the glass-to-fluid transition of the solvent. The physical origin of the shift can be explained in the context of Figure 1 and the model described in the Introduction. At temperatures below the glass-to-fluid transition, the solvent is essentially locked into the equilibrium structure appropriate for the ground state, i.e., a 2+ ion with no net dipole moment, and prevented from relaxing about the new charge distribution of the excited state. Motion along the solvent coordinate in Figure 1, therefore, does not occur on the time scale of excited-state relaxation (ca. 3 μs at 100 K). As the temperature is increased and solvent motion becomes possible, the excited-state can be stabilized relative to the Franck−Condon state via favorable solvent−solute interactions. The emission spectrum thus red-shifts through the glass-to-fluid transition, and the magnitude of this is a measure of the difference in solvation energy between the ground- and excited-state charge distributions.

To provide a means of comparing the solvent response among different compounds (and/or solvents), we introduce an expression for the normalized spectral shift, $S(T)$[30]

$$S(T) = \frac{\nu(T) - \nu(\mathrm{HT})}{\nu(\mathrm{LT}) - \nu(\mathrm{HT})} \quad (1)$$

where $\nu(T)$ is the emission maximum at temperature T and ν(LT) and ν(HT) are the emission maxima at the low- and high-temperature limits, respectively.[31] Clearly, eq 1 bears a strong resemblance to the solvent correlation function, $C(t)$, defined by others;[1,2] however, we wish to stress that with eq 1 we are *not* attempting to define a correlation function for variable-temperature spectral shifts. Spectral shifts as a function of time are, in fact, seen on a nanosecond time scale at low and intermediate temperatures for similar compounds.[32−34] Our intention with eq 1 is simply to provide a means of illustrating the temperature dependence of the emission spectra for a given compound in a concise manner. A plot of $S(T)$ for $[Ru(dmb)_3]^{2+}$ in 4:1 EtOH/MeOH is shown in Figure 2. For generation of the $S(T)$ curve, values for ν(LT) and ν(HT) were taken from the 90 and 298 K spectra, respectively. It can be seen that the function reflects the fact that the spectral evolution, resulting from changes in solvent−solute interactions to which the emission spectra are sensitive, occurs in the range 100−130 K. Below 100 K, no changes in the solvent−solute interaction are evident. Similarly, the data above 140 K do not indicate any further evolution of the system in terms of spectral position, although some intensity and bandwidth changes are apparent (vide supra). Integration of $S(T)$ yields a number we can define as the "average" temperature, $\langle T \rangle$, for the solvation response:

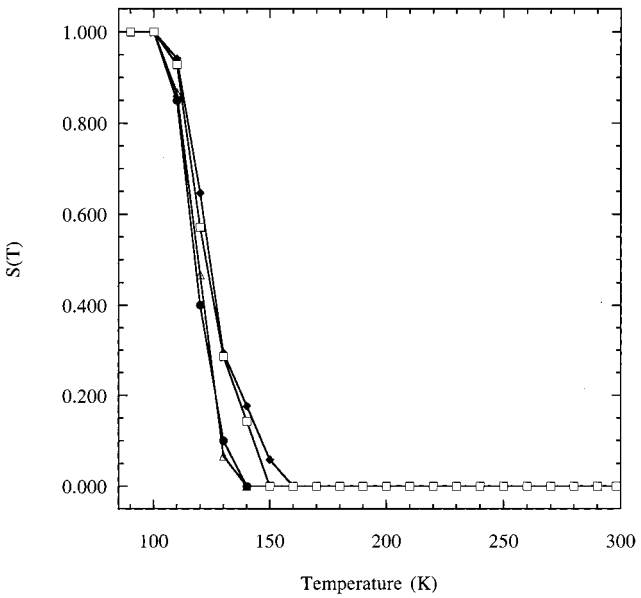

Figure 2. Plots of $S(T)$ (see eq 1) for $[Ru(dmb)_3]^{2+}$ (●), $[Ru(dpb)_3]^{2+}$ (△), $[Ru(dotb)_3]^{2+}$ (◆), and $[Ru(dmesb)_3]^{2+}$ (□) in 4:1 EtOH/MeOH.

$$\langle T \rangle = \int_{\mathrm{LT}}^{\mathrm{HT}} S(T)\, \mathrm{d}T \quad (2)$$

We expect this number to largely reflect the glassing temperature of the solvent, perturbed by the fact that $S(T)$ also contains information about larger amplitude motions associated with solvation of the ^{3}MLCT state. For $[Ru(dmb)_3]^{2+}$, we calculate $\langle T \rangle$ = 118 K, just slightly above the glassing temperature of ca. 110 K for 4:1 EtOH/MeOH.

(24) Claude, J. P. *Photophysics of Polypyridyl Complexes of Ruthenium-(II), Osmium(II), and Rhenium(I)*; University of North Carolina: Chapel Hill, NC, 1995.
(25) Casper, J. V.; Meyer, T. J. *J. Am. Chem. Soc.* **1983**, *105*, 5583.
(26) Claude, J. P.; Meyer, T. J. *J. Phys. Chem.* **1995**, *99*, 51.
(27) The intensity difference is largely due to changes in the rate of nonradiative ^{3}MLCT → $^1A_1$ decay (k_{nr}) with temperature. Although a temperature dependence of this rate is to be expected in general (cf. refs 24 and 26), it is interesting to note that the spectral intensity drops precipitously upon warming through the glass-to-fluid transition (T_g ∼ 110 K). The spectra then appear to remain essentially constant (i.e., no apparent change in k_{nr}) until approximately 250 K, at which point they begin to lose intensity again as the temperature is increased further. The increase in k_{nr} at high temperatures has been attributed for related systems to thermal population of nonemissive ligand-field excited states (e.g., $^3T_1$; cf. ref 28), and this is presumably the origin of our observations for $[Ru(dmb)_3]^{2+}$, as well. The change in nonradiative decay in the vicinity of T_g is likely a reflection of motion along the solvent coordinate as the medium passes from the glass to the fluid phase.
(28) Van Houten, J.; Watts, R. J. *J. Am. Chem. Soc.* **1976**, *98*, 4853.
(29) The structure that is introduced with decreasing temperature is also coupled to the formation of the rigid-glass medium. The featureless spectra that are generally observed for these complexes in room-temperature fluid solution arise mainly from homogeneous broadening due to the solvent. These effects are largely frozen out upon formation of a glass, and a slight enhancement in the spectral resolution results.
(30) Richert, R.; Stickel, F.; Fee, R. S.; Maroncelli, M. *Chem. Phys. Lett.* **1994**, *229*, 302.
(31) Unlike spectra obtained for compounds such as Coumarin 102, the spectra for the types of MLCT complexes studied herein are not simple Gaussian profiles. We have chosen to carry out our analyses by picking the emission maximum as the most intense feature of the vibronic progression. While it is possible to carry out spectral fitting analyses of all these spectra and extract zero-point energy differences (cf. ref 38), the models necessary for such analyses are different in different temperature regimes. This situation makes it difficult to obtain a self-consistent analysis for a data set that spans the glass-to-fluid transition. However, since the spectral shift upon melting of the glass represents a global response of all the transitions within the emission envelope, we believe that the emission maximum provides a reasonable indicator for solvent−solute interactions in these systems
(32) Kim, H. B.; Kitamura, N.; Tazuke, S. *J. Phys. Chem.* **1990**, *94*, 1414.
(33) Kim, H. B.; Kitamura, N.; Tazuke, S. *Chem. Phys. Lett.* **1988**, *143*, 77.
(34) Kitamura, N.; Kim, H. B.; Kawanishi, Y.; Obata, R.; Tazuke, S. *J. Phys. Chem.* **1986**, *90*, 1488.

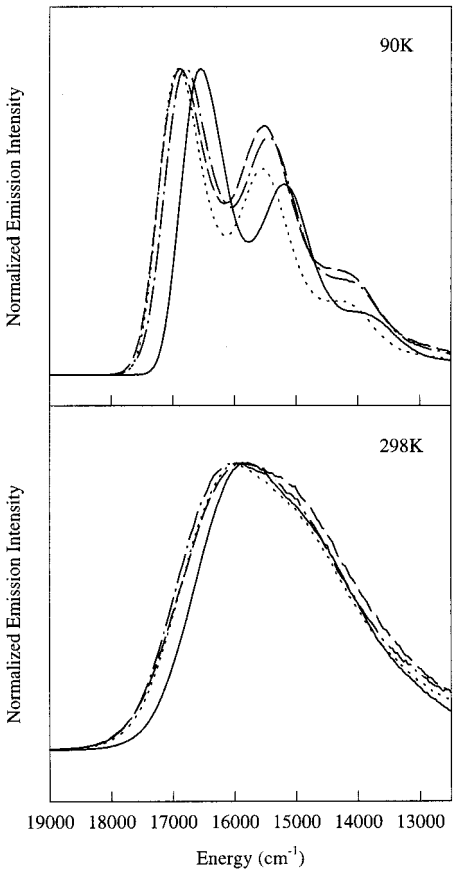

Figure 3. Emission spectra at 90 K (top panel) and 298 K (bottom panel) for $[Ru(dmb)_3]^{2+}$ (dashed), $[Ru(dpb)_3]^{2+}$ (solid), $[Ru(dotb)_3]^{2+}$ (dotted), and $[Ru(dmesb)_3]^{2+}$ (dashed−dotted) in 4:1 EtOH/MeOH.

The dpb Series. The data described above for $[Ru(dmb)_3]^{2+}$ in 4:1 EtOH/MeOH represent the basic changes in emission spectra for this class of molecules upon passing through the glass-to-fluid transition. With the dpb series, we now introduce the added perturbation of chromophore dynamics. Our previous studies of these compounds[14,22] revealed ligand-localized dynamics of the peripheral aryl rings concomitant with relaxation to the ^{3}MLCT excited state following $^1A_1 \rightarrow {}^1$MLCT excitation. In particular, ab initio and density functional calculations of models for these ligands indicated a change in the torsional angle θ of ca. 40 ± 5° for each of the three members of this series.

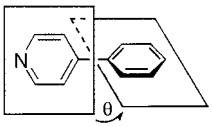

It seems reasonable to expect that these dynamics may be strongly coupled to the solvent. At temperatures below that of the glass-to-fluid transition, we expect that the rigid nature of the matrix will prevent ring rotation about θ. Thus, emission will occur from a state whose degree of electron delocalization mirrors that of the Franck−Condon state. As the temperature is increased and the matrix becomes more fluid, ring rotation will become possible and the emission spectrum will evolve toward what is seen at room temperature. Owing to the significant differences in structure among the three compounds—both in the Franck−Condon state and in the structurally relaxed ^{3}MLCT state—it was of interest to see whether the structural dynamics of the chromophore would be reflected in the variable-temperature solvent response.

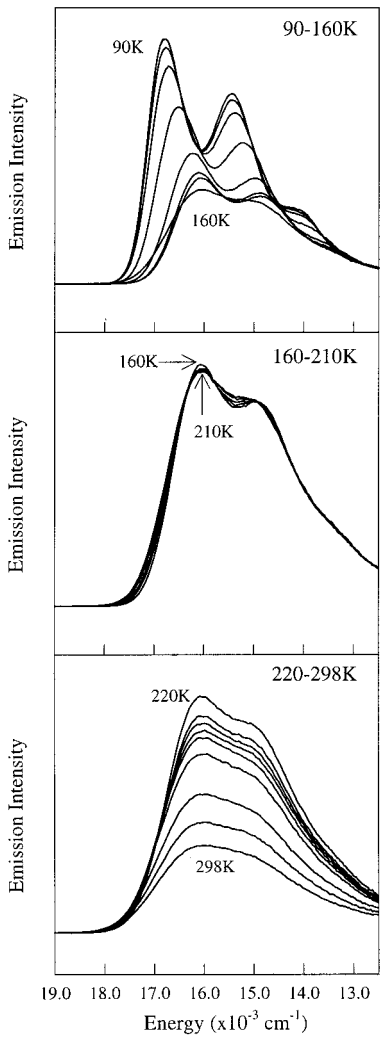

Figure 4. Emission spectra for $[Ru(dmesb)_3]^{2+}$ in 4:1 EtOH/MeOH as a function of temperature: Top panel, 90−160 K (ΔT = 10 K); middle panel, 160−210 K (ΔT = 10 K); bottom panel, 220−290 K (ΔT = 10 K) and 298 K.

In Figure 3 is shown a superposition of the 90 K spectra (top panel) and the 298 K spectra (bottom panel) of the entire series, including $[Ru(dmb)_3]^{2+}$. It is clear from these spectra that there are slight differences in the energetics of emission for this series. However, these differences are not nearly as pronounced as might have been expected, given the significant differences in ground-state structures. For example, there is a striking similarity between the $[Ru(dmb)_3]^{2+}$ and $[Ru(dmesb)_3]^{2+}$ spectra despite the different structures of these two compounds. In Figure 4 is shown a plot of variable-temperature emission spectra for $[Ru(dmesb)_3]^{2+}$; plots of $S(T)$ for all members of the series are illustrated in Figure 2. In general, we observe no significant differences among any of the four molecules in their spectral profiles with changes in temperature. There are slight changes in $S(T)$, and the curve is somewhat broader for the arylated compounds relative to $[Ru(dmb)_3]^{2+}$. The degree of broadening appears to increase with the addition of steric bulk, with $[Ru(dotb)_3]^{2+}$ and $[Ru(dmesb)_3]^{2+}$ showing the most pronounced effect. Application of eq 2 to the $[Ru(dmesb)_3]^{2+}$ data yields a value of $\langle T \rangle = 124$ K, suggesting that while a difference between $[Ru(dmb)_3]^{2+}$ and $[Ru(dmesb)_3]^{2+}$ does exist, it is a relatively minor effect. Any differences that do exist across the series are largely washed out through the glass-to-fluid transition of the solvent. The 298 K spectra are very similar to those we

previously reported in acetonitrile,[14] and as such, they reflect the expected extent of excited-state delocalization that is sterically allowed (i.e., slight red-shifting of the $[Ru(dpb)_3]^{2+}$ spectrum concomitant with a narrow emission band.) It is therefore likely that the red shift of the $[Ru(dpb)_3]^{2+}$ spectrum with respect to those of the other species at 90 K (Figure 3) is less a property of solvation and more a result of excited-state delocalization allowed in the ground-state structure of this molecule. On the basis of these observations, we conclude that solvation by 4:1 EtOH/MeOH is relatively insensitive to chromophore structural dynamics through the glass-to-fluid transition in this series of compounds. This was initially surprising; however, the similarity of the solvent response for these four structurally disparate molecules can be rationalized on the basis of the likely solvation structure surrounding the chromophores. Following the MLCT excitation, each compound has a dipole with its negative end pointing directly at the first solvation shell. The need to essentially invert the nature of the solvent structure from one appropriate for a cation (ground state) to one appropriate for an anion (excited state) is likely to be an important factor driving solvation dynamics in these systems. In general, we would expect this to require a substantial change in the solvent structure about the chromophore. However, in the case of solvation by a protic solvent such as an alcohol, the necessary change may only involve rotation about the C−O bond. The small-amplitude motion needed to achieve charge stabilization of the MLCT state suggested by this model could therefore make 4:1 EtOH/MeOH (and other sterically nondemanding alcohols in general) relatively insensitive to chromophore structure.

II. Solvation Properties of 2-MeTHF. Variable-Temperature Studies of $[Ru(dmb)_3]^{2+}$. To determine whether the results in 4:1 EtOH/MeOH were indicative of generally weak coupling between chromophore structural dynamics and solvation in these systems, we carried out analogous studies of these four molecules in 2-MeTHF. This solvent was chosen in part because it has the ability to form good-quality optical glasses but, more importantly, because it is an aprotic solvent that will likely require larger amplitude motion in response to a change in the sign of the solvated charge density. As before, we start with $[Ru(dmb)_3]^{2+}$, since this provides information on the solvent response in the absence of chromophore structural dynamics. An overlay of spectra collected in 2-MeTHF and 4:1 EtOH/MeOH at 90 K can be found in the Supporting Information. The spectra are virtually superimposable, suggesting that solvation about the chromophore is very similar in these two media at 90 K.

However, this similarity is not retained upon increasing the temperature. Figure 5 clearly reveals the profound differences between these two solvent systems. The most remarkable feature of the 2-MeTHF solvent response curve is that the emission spectrum of $[Ru(dmb)_3]^{2+}$ initially red-shifts through the glass-to-fluid transition but then undergoes a significant *blue* shift as the temperature is increased further. The overall solvent response thus extends to about 200 K, far beyond the region of the glass-to-fluid transition at ca. 90 K.[35] The maximum breadth in spectral shift is ca. 1000 cm^{-1} between 90 K (16 800 cm^{-1}) and ca. 130 K (15 800 cm^{-1}), the same magnitude observed in 4:1 EtOH/MeOH. The subsequent blue shift recovers 200 cm^{-1} of this, making the ν(LT) − ν(HT) differential 800 cm^{-1}. The blue shift is therefore quite significant, corresponding to 20% of the overall difference in solvation energies between the

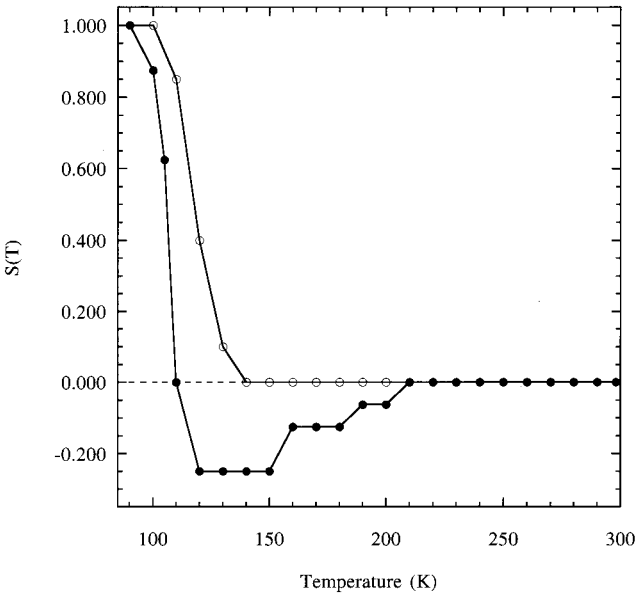

Figure 5. Plots of $S(T)$ for $[Ru(dmb)_3]^{2+}$ in 2-MeTHF (●) and 4:1 EtOH/MeOH (○).

Franck−Condon configuration of the solvent and the fully relaxed ^{3}MLCT state. Recently, Görlach et al.[36] described the static and time-dependent fluorescence spectroscopy of the organic dye oxazine-4 in 2-MeTHF over the temperature range 80−250 K. Included in their report was a plot of the position of the $S_1(\nu' = 0) \rightarrow S_0(\nu'' = 0)$ emissive transition as a function of temperature where they observe the same phenomenon as we have described for $[Ru(dmb)_3]^{2+}$: the spectrum exhibits a maximum of 16 300 cm^{-1} at 80 K, red-shifts to just below 15 800 cm^{-1} by 140 K, then blue-shifts by >100 cm^{-1} to about 15 900 cm^{-1} by 250 K. These authors do not comment on this aspect of their data, but these results and the marked dissimilarity between the electronic structures of oxazine-4 and $[Ru(dmb)_3]^{2+}$ clearly suggest that some property of 2-MeTHF is likely responsible for the observations illustrated by Figure 5.

We believe the shift that occurs above the glass-to-fluid transition in the emission spectra of both $[Ru(dmb)_3]^{2+}$ and oxazine-4 is a manifestation of the temperature dependence of the polarity and polarizability of 2-MeTHF. This effect was recently described in detail by Bublitz and Boxer.[37] Their analysis reveals that, in addition to an overall contraction of a given solvent with decreasing temperature, the presence of a dipole in the solute will orient solvent molecules in the vicinity of the solute. This effect will become more pronounced as the temperature is lowered due to the reduction in thermal fluctuations of the solvent molecules, resulting in an increase in the effective polarity of the solvent with decreasing temperature. It is important to note that this model describes a localized effect; i.e., only solvent molecules near the dipolar solute will be significantly affected. Such local changes will not be reflected in the bulk dielectric properties measured for the pure solvent as a function of temperature but will be extremely important in terms of the energetics of solute−solvent interactions.

The application of this model to our data is most easily described by considering the spectral shift as a function of decreasing temperature. At room temperature, solvation dynamics are much faster than excited-state relaxation: the 2-MeTHF molecules are therefore solvating the excited-state dipole present

(35) Mizukami, M.; Fujimori, H.; Oguni, M. *Prog. Theor. Phys. Suppl.* **1997**, 79.

(36) Görlach, E.; Gygax, H.; Lubini, P.; Wild, U. P. *Chem. Phys.* **1995**, *194*, 185.

(37) Bublitz, G. U.; Boxer, S. G. *J. Am. Chem. Soc.* **1998**, *120*, 3988.

in the ^{3}MLCT excited state. As the temperature is lowered, the solvent contracts and, more importantly, becomes more ordered around the excited-state dipole of the solute. The resulting increase in effective polarity of the solvent translates into an increase in the degree of stabilization energy afforded by the solvent and is manifested as a red shift of the emission maximum. In terms of Figure 1, the effect is a reduction in the zero-point energy of the excited state relative to that of the ground state, i.e., vertical motion of the entire excited-state potential energy surface as opposed to the horizontal motion along the solvent coordinate we have been discussing thus far. This red shift continues as the temperature is lowered further until the solvent begins to glass, whereupon the spectrum begins to blue-shift due to hindered motion along the horizontal axis of Figure 1 as described previously. The reason a similar temperature-dependent effect is not seen in the 4:1 EtOH/MeOH data[38] is likely that polar solvents such as alcohols are already ordered at room temperature. Thus, the difference in solvent structure (and therefore solvation energy) is less pronounced with a change in temperature than for less polar solvents such as 2-MeTHF.[37]

The dpb Series in 2-MeTHF. Low-Temperature Spectra. Comparison of the spectra collected at 90 K for the three arylated compounds (Figure 6, top) indicates that there are profound differences in the energy of the emissive species across this series in 2-MeTHF. Specifically, the data reveal a substantial blue shift in the emission maximum as steric bulk on the aryl substituent is increased, from 16 600 cm^{-1} for $[Ru(dpb)_3]^{2+}$ to 17 300 cm^{-1} for $[Ru(dmesb)_3]^{2+}$. The same effect is not observed from a comparison of the 90 K spectra of the three compounds in 4:1 EtOH/MeOH (Figure 3). The bottom panel in Figure 6 shows an overlay of the 90 K spectra for $[Ru(dmesb)_3]^{2+}$ in 4:1 EtOH/MeOH and 2-MeTHF. Again, a significant blue shift is noted, this time for a common luminophore.[39] It can therefore be concluded that the blue shift revealed by the spectra in the top panel of Figure 6 is indicative of differences in the nature of solvation by 2-MeTHF across the dpb series.

We believe the physical origin of the blue shift across the dpb series revealed in Figure 6 (top) is, in fact, related to structure-specific solvent−solute interactions. As revealed in our earlier work on these systems,[14,22] introduction of methyl substituents causes an increase in the dihedral angle θ between the pyridyl and peripheral aryl rings (vide supra). With regard to solvation, this has two important consequences. First, as the dihedral angle increases in the ground state from ca. 45° in $[Ru(dpb)_3]^{2+}$ to ∼90° in $[Ru(dmesb)_3]^{2+}$, electron density in the Franck−Condon state becomes more localized in the bipyridyl rings. The resulting decrease in conjugation onto the aryl substituent implies less excited-state charge density on the portion of the molecule that interacts most strongly with the solvent.[22] Second, a steric effect due to the introduction of methyl groups ortho to the C−C link occurs concomitantly with this shift in electron density inward toward the bipyridyl fragment. As θ increases, these methyl groups will be located above and/or below the plane of the bipyridine, thereby restricting solvent access to the excited-state charge density. Combining these two effects, we can expect that, as steric bulk is added to the aryl substituents, the ability of 2-MeTHF to interact with, and solvate, the charge density associated with the MLCT state will be hindered.

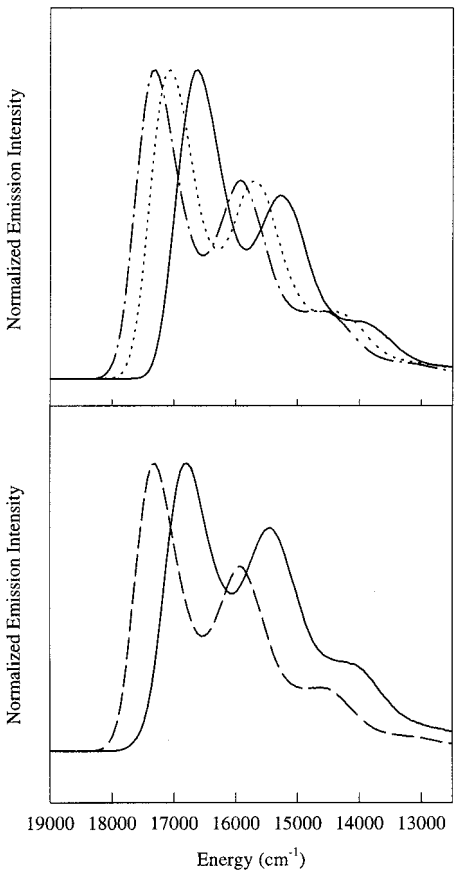

Figure 6. Top panel: Emission spectra at 90 K for $[Ru(dpb)_3]^{2+}$ (solid), $[Ru(dotb)_3]^{2+}$ (dotted), and $[Ru(dmesb)_3]^{2+}$ (dashed−dotted) in 2-MeTHF. Bottom panel: Emission spectra at 90 K for $[Ru(dmesb)_3]^{2+}$ in 4:1 EtOH/MeOH (solid) and 2-MeTHF (dashed).

Using this model, we can understand the trends in the 90 K emission spectra observed across the dpb series in 2-MeTHF. In the case of $[Ru(dpb)_3]^{2+}$, the minimal steric constraints of the ligand result in fairly extensive conjugation between the aryl substituent and the bipyridyl fragment. This allows for significant delocalization of charge density in the Franck−Condon state onto the peripheral aryl rings penetrating the solvent.[22] In addition, the absence of methyl group steric bulk allows the solvent easier access to the cationic core of the molecule. When the excited-state dipole is formed, there is therefore the possibility for extensive solvent−solute interactions. $[Ru(dmesb)_3]^{2+}$, however, contains two methyl groups for each aryl substituent. In addition to sterically restricting access of the solvent to the core of the molecule in terms of

(38) Claude and Meyer (cf. refs 24 and 26) have reported an increase in the energy gap E_0 with temperature for Re(I) and Os(II) systems as well as for $[Ru(bpy)_3]^{2+}$ in 4:1 EtOH/MeOH after the glass-to-fluid transition. They have shown that this effect is due to an entropic increase in the solvent−solute system as the temperature is raised, reflecting frequency changes in solvent librations. We have stated that the variable-temperature emission data for $[Ru(dmb)_3]^{2+}$ in 4:1 EtOH/MeOH are similar to those collected for $[Ru(bpy)_3]^{2+}$ in 4:1 EtOH/MeOH, and yet we report no blue shift for our data (Figure 2). This apparent inconsistency arises because we have used the emission maximum as a marker of spectral shifting over the entire temperature range whereas Claude and Meyer have used spectral fitting to determine values for E_0 in a temperature regime after the glass-to-fluid transition where a single-mode spectral fitting analysis is valid (cf. ref 31). However, the fact that a blue shift is readily apparent for $[Ru(dmb)_3]^{2+}$ in 2-MeTHF (Figure 5) using the emission maximum as a marker of spectral shifting is indicative of the significant difference in the variable-temperature solvation properties of 2-MeTHF versus 4:1 EtOH/MeOH.

(39) The fact that the absorption spectra of a given chromophore (e.g., $[Ru(dmesb)_3]^{2+}$) are essentially superimposable in the two solvent systems (see Supporting Information) indicates that solvation differences are largely the result of interactions with the excited-state charge density distribution.

ground-state solvation, the large dihedral angle induced between the π systems of the pyridyl and mesityl rings results in significant attenuation of excited-state charge density on the aryl substituent in the Franck−Condon state. The net effect is a reduction in the degree of interaction between the solvent and the charge density associated with the MLCT excited state. $[Ru(dotb)_3]^{2+}$, then, represents the intermediate case where the increased dihedral angle relative to $[Ru(dpb)_3]^{2+}$ means a reduction in charge density on the aryl substituents in the Franck−Condon state, but not to the extent expected for $[Ru(dmesb)_3]^{2+}$. In addition, the CH_3 group serves to partially hinder access by the solvent to the cationic core, resulting in a smaller degree of solvent−solute interactions than found for $[Ru(dpb)_3]^{2+}$. However, the presence of only one CH_3 group indicates that one face of the ligand system should be sterically unencumbered. The overall solvent−solute interaction is more extensive than that for $[Ru(dmesb)_3]^{2+}$ and results in a smaller blue shift. The reason a similar trend was not observed for the compounds dissolved in 4:1 EtOH/MeOH is likely that small, rod-shaped linear-chain alcohols such as MeOH and EtOH are not as sterically demanding as the larger and more spherically shaped 2-MeTHF.

Regardless of the specific details of the description of the solvent structure at 90 K, it is clear from the low-temperature emission spectra that there is structural specificity in the solvent−solute interaction between compounds in the dpb series and 2-MeTHF. Such discrimination has a significant and measurable effect on the energetics of the Franck−Condon state and, presumably, on the structure of the solvent shell surrounding the compound. Given that we know the structures of these chromophores change dramatically over the course of excited-state evolution, the question arises as to whether the sensitivity of 2-MeTHF to chromophore structure will be reflected in the dynamics of solvation.

Variable-Temperature Spectra of $[Ru(dpb)_3]^{2+}$ in 2-MeTHF. As the simplest case, we examine first the emission spectra of $[Ru(dpb)_3]^{2+}$ as a function of temperature. In Figure 7 are plotted spectra collected in the range 90−298 K; the corresponding plot of $S(T)$ is given in Figure 8. The overall shapes of the emission spectra at each temperature, as well as the qualitative appearances of the spectra as functions of temperature, are reminiscent of what is seen for this compound in 4:1 EtOH/MeOH. In addition, changes in the spectra at lower temperatures (i.e., up to ca. 120 K) are very similar to what was observed for $[Ru(dmb)_3]^{2+}$ in 2-MeTHF. The difference in the behavior of this system versus $[Ru(dmb)_3]^{2+}$ in 2-MeTHF is made clear upon examination of the plot of $S(T)$. Following an initial steep drop in $S(T)$ through the high-temperature portion of the glass-to-fluid transition, changes in the spectra continue in a very gradual sense throughout the entire temperature range studied. The overall shift in the spectrum is ca. 1300 cm^{-1} — much larger than what was observed for the same compound in 4:1 EtOH/MeOH — and is not complete until 260 K. In the absence of a phenyl substituent, i.e., for $[Ru(dmb)_3]^{2+}$, the data show an initial red shift through the glass-to-fluid transition, followed by a blue shift. In Figure 8, we see that no such blue shift is apparent for $[Ru(dpb)_3]^{2+}$. Assuming that the blue shift seen for $[Ru(dmb)_3]^{2+}$ is a property of the solvent, we can infer that a similar blue shift in the $[Ru(dpb)_3]^{2+}$ data is being obscured in the higher temperature region.

It is difficult to know precisely what is occurring at the molecular level in terms of the coupling of aryl ring rotation and the 2-MeTHF solvent molecules as a function of temperature. However, we speculate that several factors may be

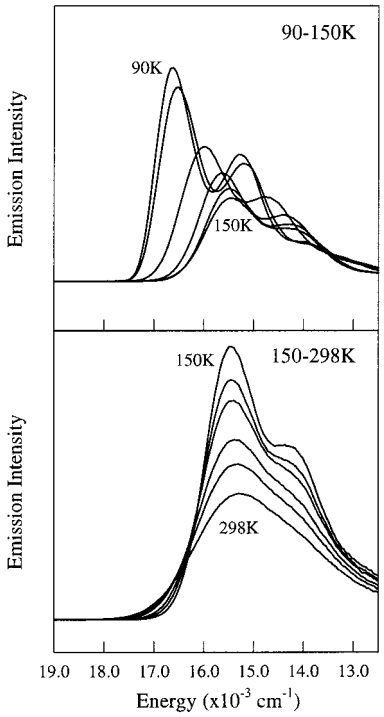

Figure 7. Emission spectra for $[Ru(dpb)_3]^{2+}$ in 2-MeTHF as a function of temperature: top panel, 90−130 K ($\Delta T = 10$ K) and 150 K; bottom panel, 150, 170, 190, 230, 260, and 298 K.

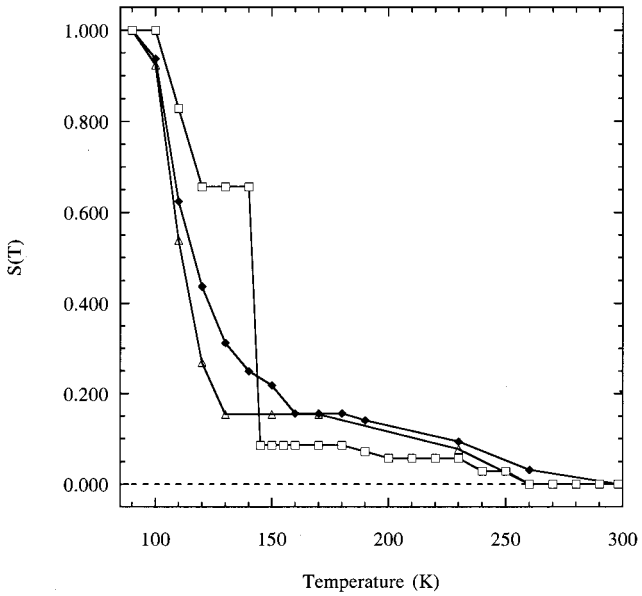

Figure 8. Plots of $S(T)$ for $[Ru(dpb)_3]^{2+}$ (△), $[Ru(dotb)_3]^{2+}$ (◆), and $[Ru(dmesb)_3]^{2+}$ (□) in 2-MeTHF.

important. The first relates to the large-amplitude motion of the aryl ring itself and the solvent's response to that motion. It is known that the phenyl ring in $[Ru(dpb)_3]^{2+}$ undergoes a rotation of ca. 45° in the course of excited-state thermalization.[14,22] At low temperature (e.g., <100 K), the rigid nature of the solvent matrix hinders this motion. As the temperature is increased, the ring will begin to rotate as motion through the solvent becomes possible. However, this process requires significant displacement of solvent molecules and should therefore be affected by the viscosity of the medium. In comparing $[Ru(dpb)_3]^{2+}$ and $[Ru(dmb)_3]^{2+}$, it seems reasonable to expect that the temperature dependence of the viscosity of 2-MeTHF would significantly affect the solvation dynamics of $[Ru(dpb)_3]^{2+}$, where there is a

large degree of molecular motion associated with excited-state evolution.[21] This could explain at least in part the differences in $S(T)$ between these compounds. A second factor concerns the probable motion of the 2-MeTHF molecules in response to the change in charge density of the luminophore. We indicated earlier that the cationic nature of these compounds means that the ground-state solvation shell is one in which the negative ends of the solvent dipoles are pointed toward the metal complex. In the case of 2-MeTHF, this corresponds to the oxygen atom. The MLCT excited state reverses the sign of the charge density of the metal complex, at least in the region of charge-transfer localization. However, in contrast to the case of alcoholic solvents, we expect that much larger amplitude motion of the 2-MeTHF molecule will be required to restore a more favorable solvent−solute interaction in the excited state. While the exact nature of this motion is difficult to specify, the most likely change would seem to involve at least a partial rotation of the solvent molecules such that the lone pairs of the oxygen are pointed away from the bpy^- fragment. Finally, as ring rotation proceeds, the degree of excited-state electronic delocalization increases and 2-MeTHF must also respond to this time/temperature-dependent change in the charge density distribution within the solute.

Variable-Temperature Spectra of $[Ru(dmesb)_3]^{2+}$ in 2-MeTHF. The most sterically demanding of the molecules in the series is $[Ru(dmesb)_3]^{2+}$. Plots of the emission spectra of $[Ru(dmesb)_3]^{2+}$ in 2-MeTHF as a function of temperature are shown in Figure 9, with a plot of $S(T)$ given in Figure 8. Initially, we observe a smaller shift in the emission spectrum through the glass-to-fluid transition than was seen for the previous molecules. The relatively small spectral shift ceases altogether at 120 K with the emission maximum remaining constant until a sharp transition in the 140−145 K range. At this point, the peak of the spectrum shifts several hundred reciprocal centimeters to the red over a very small temperature interval. Following this, the spectral evolution begins to take on a character reminiscent of what was observed for $[Ru(dpb)_3]^{2+}$. The sharp discontinuity in the data is remarkable and occurs at a temperature (ca. 145K) well above the glass-to-fluid transition of the pure solvent. We note that the vibrational spacings obtained from spectral fitting analyses above and below the transition temperature are essentially identical, suggesting that the intramolecular nature of the emission is not changing in the course of the spectral evolution. On the basis of this, the anomalous appearance of the variable-temperature emission spectra of $[Ru(dmesb)_3]^{2+}$ in 2-MeTHF would appear to arise from a transition between two luminophores differing largely in the nature of their solvation.

Our interpretation of the data shown in Figure 9 is as follows. As stated, the ground-state structure of $[Ru(dmesb)_3]^{2+}$ is one in which the mesityl−pyridyl dihedral angle is large and the 90 K spectrum was interpreted as reflecting an inability of the 2-MeTHF molecules to effectively solvate the Franck−Condon state due to a combination of sterics and the limited extent of electron delocalization onto the peripheral aryl ring. As the temperature is increased above the glass-to-fluid transition temperature, significant movement of the aryl rings requires displacement of 2-MeTHF molecules. This amounts to a barrier for excited-state evolution involving aryl ring rotation. We suggest that this barrier is more significant in $[Ru(dmesb)_3]^{2+}$ than for $[Ru(dpb)_3]^{2+}$ due to the added steric bulk on the aryl ring. We believe that the transition beginning near 140 K corresponds to that point at which this barrier is overcome due to the drop in solvent viscosity expected with increasing

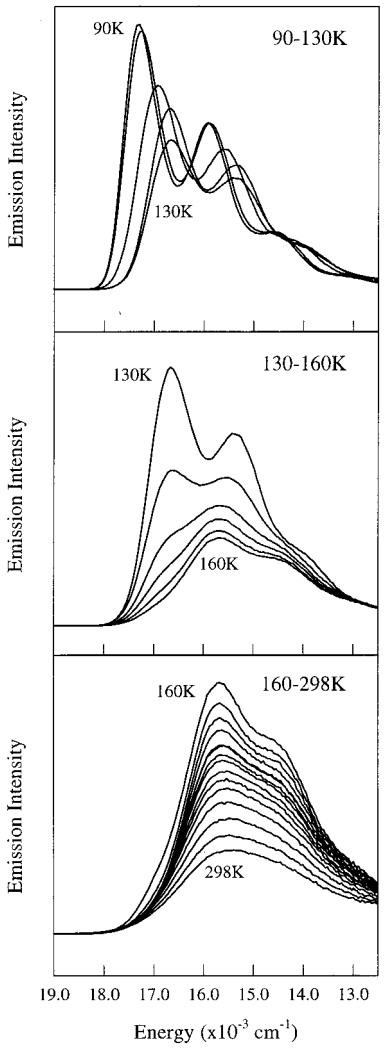

Figure 9. Emission spectra for $[Ru(dmesb)_3]^{2+}$ in 2-MeTHF as a function of temperature: top panel, 90−130 K (ΔT = 10 K); middle panel, 130−160 K (ΔT = 10 K), 145 K, and 155 K; bottom panel, 160−290 K (ΔT = 10 K) and 298 K.

temperature. The result is a rapid transition that allows solvent access to the excited-state charge density in the bipyridyl plane due to both displacement of the CH_3 groups and to the concomitant increase in charge density on the peripheral aryl ring. The system then evolves much the same way as $[Ru(dpb)_3]^{2+}$ with further increases in temperature. The process we are proposing can be depicted in a potential energy surface diagram such as that illustrated in Figure 10. The x axis corresponds to a generalized solvent−solute interaction coordinate, whereas the y axis is the energy of the luminophore and its associated solvation shell. Emission at temperatures below 135 K is believed to come out of the upper potential surface, where little change in the solvent−solute interaction occurs even after the glass melts due to the (relatively) unperturbed structure of the system (i.e., $\Delta Q \sim 0$). As the temperature is raised, a barrier is crossed corresponding to motion of the aryl substituent that results in a drastic change in the solvent−solute interactions. The subsequently red-shifted emission arises out of the lower energy potential surface, one more reminiscent of what likely exists for $[Ru(dpb)_3]^{2+}$ in fluid 2-MeTHF. It is impossible at present to state the exact microscopic nature of such a barrier between two potential energy surfaces. We note, however, that if solvent motion and intramolecular ring rotation are occurring

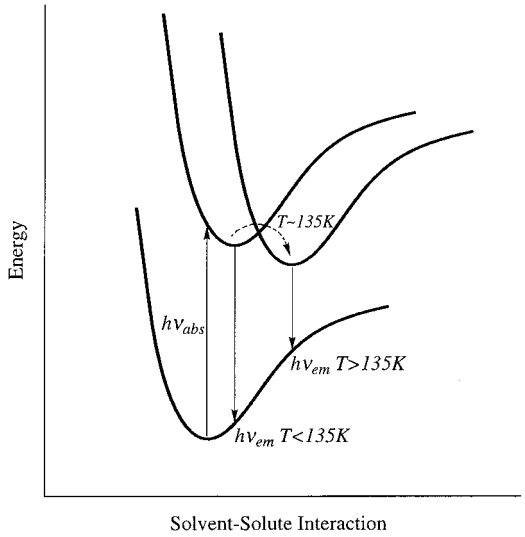

Figure 10. Proposed potential energy surface diagram for the solvent−solute interaction coordinate seen for $[Ru(dmesb)_3]^{2+}$ in 2-MeTHF as a function of temperature. See text for details.

together on the time scale of radiative transitions at these intermediate temperatures, then the ensemble would effectively have two competing luminescence states. Single-wavelength nanosecond emission lifetime measurements reveal complex dynamics as a function of temperature. However, this is not unique to this system and spectral shifting that occurs concomitant with excited-state relaxation makes interpretation of these observations difficult. A more extensive full-spectrum study of temperature-dependent emission dynamics is planned for the near future.

Temperature-dependent fluorescence data for $[Ru(dotb)_3]^{2+}$ indicate a solvent−solute interaction condition intermediate between that of $[Ru(dpb)_3]^{2+}$ and $[Ru(dmesb)_3]^{2+}$. A plot of $S(T)$ for this system is also given in Figure 8. The Franck−Condon state, consisting of a canted structure with $\theta \sim 65°$,[22] will have a charge density that is both partially obstructed from the solvent and partially accessible, resulting in its intermediate position in the 90 K spectral plot in Figure 7. Employing our viscosity model, we expect that the presence of a single CH_3 group will increase the viscous drag of this system relative to that of $[Ru(dpb)_3]^{2+}$ but be attenuated relative to $[Ru(dmesb)_3]^{2+}$. The barrier to ring rotation should therefore energetically lie between those of $[Ru(dpb)_3]^{2+}$ and $[Ru(dmesb)_3]^{2+}$. The plot of $S(T)$ appears to conform to this picture, at least qualitatively: the glass-to-fluid transition brings about a red shift similar to that of $[Ru(dpb)_3]^{2+}$, but is much broader in terms of its thermal range. However, the transition in $[Ru(dotb)_3]^{2+}$ falls short of actually becoming trapped in the upper potential surface depicted in Figure 10 as occurred in the case of $[Ru(dmesb)_3]^{2+}$.

Concluding Comments

We have presented variable-temperature static emission spectra for a series of aryl-substituted bipyridyl complexes of Ru^{II} in an effort to explore issues relating to solvation dynamics in the excited-state evolution of transition metal complexes. The values of radiative decay (k_r) are typically too small in such systems to carry out the requisite time-resolved measurements to detail solvent response. Despite this, we have taken advantage of the conceptual link one can make between time and temperature and discovered some of the important factors that influence solvation in MLCT excited-state formation and decay. Specifically, for the case of $[Ru(dmb)_3]^{2+}$, $[Ru(dpb)_3]^{2+}$, $[Ru(dotb)_3]^{2+}$, and $[Ru(dmesb)_3]^{2+}$, significant differences are noted in the variable-temperature emission properties for this series of compounds dissolved in 4:1 EtOH/MeOH versus 2-MeTHF. While the solvation response of 4:1 EtOH/MeOH appears to be essentially insensitive to chromophore structure, data collected in 2-MeTHF vary enormously both qualitatively and quantitatively in response to the changing steric requirements and intramolecular relaxation dynamics across the series. While specific origins for the differences across the series in 2-MeTHF are not completely clear, we believe these results are indicative of the potential importance of structure-specific solvent−solute interactions in the dynamics of solvation, particularly in systems for which large-amplitude molecular motion accompanies excited-state evolution.

One final point we wish to make concerns the extent to which we can correlate the temperature dependence of solvation we have presented here with ultrafast studies of solvent dynamics conducted at room temperature. Although one can think of low-temperature excited-state behavior in analogy to short time scale behavior, we have stopped short of suggesting a quantitative connection between these two domains. Some of the difficulties with making such a correlation are as follows: First, as indicated from the data we obtained for $[Ru(dmb)_3]^{2+}$ in 2-MeTHF, there is a significant difference in the polarity and polarizability of medium dielectric solvents between low and high temperature—such is not the case for a solvent at a single temperature as a function of time. Second, intermolecular interactions can vary significantly as a function of temperature, much less so as a function of time. Third, the viscosities of solvents are highly temperature dependent and can strongly influence coupling between solvent and solute dynamics. Again, this is likely to be less important at a single temperature in the time domain. It may be possible to quantify the time/temperature connection further through time-dependent studies of spectral evolution, and this aspect of the problem is currently being explored. Given the formidable problems associated with ultrafast studies of solvation dynamics with relatively weakly emissive compounds, however, we believe the present study has demonstrated that variable-temperature static spectroscopic measurements can provide insight into the solvation processes occurring in such systems.

Acknowledgment. The authors to thank Professors Mark Maroncelli and Graham Fleming for helpful discussions. This research was supported by the U.S. Department of Energy, Office of Basic Energy Sciences, Division of Chemical Sciences (Grant No. DE-FG03-96ER14665) and the Alfred P. Sloan Foundation.

Supporting Information Available: Emission spectra for $[Ru(dmb)_3]^{2+}$ in 4:1 EtOH/MeOH as a function of temperature, emission spectra at 90 K for $[Ru(dmb)_3]^{2+}$ in 4:1 EtOH/MeOH and 2-MeTHF, and room-temperature absorption spectra of $[Ru(dmesb)_3]^{2+}$ in 4:1 EtOH/MeOH and 2-MeTHF. This material is available free of charge via the Internet at http://pubs.acs.org.

IC990703L